Geosci. Model Dev. Discuss., 8, 3971–4018, 2015
www.geosci-model-dev-discuss.net/8/3971/2015/
doi:10.5194/gmdd-8-3971-2015

Geoscientific Model Development Discussions
Open Access

S^4CAST v2.0: sea surface temperature based statistical seasonal forecast model

R. Suárez-Moreno[1,2] and B. Rodríguez-Fonseca[1,2]

[1]Departamento de Geofísica y Meteorología, Facultad de Físicas, Universidad Complutense de Madrid, Plaza de las Ciencias 1, 28040 Madrid, Spain
[2]Instituto de Geociencias (IGEO), Facultad de Ciencias Geológicas, Universidad Complutense de Madrid – CSIC, C/José Antonio Novais 12, 28040 Madrid, Spain

Received: 12 March 2015 – Accepted: 27 April 2015 – Published: 26 May 2015

Correspondence to: R. Suárez-Moreno (roberto.suarez@fis.ucm.es)

Published by Copernicus Publications on behalf of the European Geosciences Union.

Abstract

Sea Surface Temperature is the key variable when tackling seasonal to decadal climate forecast. Dynamical models are unable to properly reproduce tropical climate variability, introducing biases that prevent a skillful predictability. Statistical methodologies emerge as an alternative to improve the predictability and reduce these biases. Recent studies have put forward the non-stationary behavior of the teleconnections between tropical oceans, showing how the same tropical mode has different impacts depending on the considered sequence of decades. To improve the predictability, the Sea Surface Temperature based Statistical Seasonal foreCAST model (S^4CAST) introduces the novelty of considering the non-stationary links between the predictor and predictand fields. This paper describes the development of S^4CAST model whose operation is focused on the study of the predictability of any variable related to sea surface temperature. An application focused on West African rainfall predictability has been implemented as a benchmark example.

1 Introduction

Global oceans have the capacity of storage heat and release it as energy that is transferred to the atmosphere altering global atmospheric circulation. Therefore, fluctuations in monthly sea surface temperature (SST) may be considered as an important source of seasonal predictability, improving the ability to forecast climate variables. Many research works have been conducted to study the impacts of worldwide sea surface temperature anomalies (SSTA) by means of dynamical models, observational studies and statistical methods. In this way, tropical oceans purchase greater relevance (Rasmusson and Carpenter, 1982; Harrison and Larkin, 1998; Klein et al., 1999; Saravanan and Chang, 2000; Trenberth et al., 2002; Chang et al., 2006; Ding et al., 2012; Wang et al., 2012; Ham, 2013a, b; Keenlyside et al., 2013). Because of the persistence shown by SSTA, alterations that occur in the oceans are slower than changes occurring in the

GMDD
8, 3971–4018, 2015

S^4CAST seasonal forecast model

R. Suárez-Moreno and B. Rodríguez-Fonseca

atmosphere. Once the thermal equilibrium between the ocean and the atmosphere is broken, oceans are able to release its energy, changing the atmospheric circulation for some time before dissipating, leading in turn to an influence on other variables, being the SSTA a potential predictor of their anomalous behavior.

The links between SST variability and rainfall have been documented by works dealing with the influence of tropical SST on seasonal precipitation regimes that mainly occur in India and West Africa (Ward, 1998; Rasmusson and Carpenter, 1983; Ashok et al., 2001; Kucharski et al., 2008; Rodríguez-Fonseca et al., 2011; Mohino et al., 2011). Particularly, for the West African Monsoon (WAM), the SSTA becomes the main source of predictability (Folland, 1986; Palmer, 1986; Fontaine et al., 1998; Rodríguez-Fonseca et al., 2015). On the one hand, SSTA is presented as the main driver of the decadal variability (Janicot et al., 2001; Biasutti et al., 2008; Martin and Thorncroft, 2013). On the other hand, several observational studies suggest the influence of global SSTA on the WAM at interannual time scales, pointing to changes associated with El Niño-southern Oscillation (ENSO) (Janicot et al., 2001; Rowell, 2001; Joly and Voldoire, 2009), the Atlantic Niño (Giannini et al., 2003; Polo et al., 2008; Joly and Voldoire, 2009; Nnamchi and Li, 2011), the Mediterranean (Rowell, 2003; Gaetani et al., 2010; Fontaine et al., 2011) and the Indian Ocean (Chung and Ramathan, 2006; Lu, 2009) all identified by their impact on the monsoon system and its predictability. Beyond Indian monsoon and WAM, there are studies on the influence of the SSTA on rainfall throughout the Americas (Shin and Sardeshmukh, 2010; Giannini et al., 2001; Haylock et al., 2006), Europe (Bulic and Kucharski, 2012; López-Parages and Rodríguez-Fonseca, 2012) or even Australia (Drosdowsky and Chambers, 2001) among others.

The study of the impacts of tropical global SST on climate has become increasingly important during the last decades. Thus, there are dynamical and statistical prediction models that attempt to define and predict seasonal averages from interannual to multidecadal time scales. In this way, General Circulation Models (GCMs) emerged from the need to reproduce the ocean–atmosphere interactions, responsible for much of climate variability whose major component is attributed to ENSO phenomenon (Bjerknes, 1969; Gill, 1980). Numerous research centers worked extensively to create their own models from coupled ocean–atmosphere GCMs used in conjunction with statistical methods to achieve reliable ENSO variability predictions and analyze the skill of these models (Cane et al., 1986; Barnett and Preisendorfer, 1987; Zebiak and Cane, 1987; Barnston and Ropelewski, 1992; Barnett et al., 1993; Barnston et al., 1994, 1999; Ji et al., 1994a, b; Van den Dool, 1994; Mason et al., 1999). Predictability of rainfall has become a scope for these models, finding works that have focused on this issue by means of dynamical and statistical models (Garric et al., 2002; Coelho et al., 2006). However, the difficulty of GCMs to adequately reproduce the tropical climate variability remains a real problem, so that in recent years the number of studies focusing on specific aspects of the biases of these models has increased exponentially (Biasutti et al., 2006; Richter and Xie, 2008; Wahl et al., 2011; Doi et al., 2012; Li and Xie, 2012, 2014; Richter et al., 2012; Bellenguer et al., 2013; Brown et al., 2013; Toniazzo and Woolnough, 2013; Vanniere et al., 2013; Xue et al., 2013).

Statistical models have been widely used as an alternative way of climate forecasting, including several techniques in their development. Model Output Statistics (MOS) determine a statistical relationship between the predictand and the variables obtained from dynamic models (Glahn and Lowry, 1972; Klein and Glahn, 1974; Vislocky and Fritsch, 1995). Stochastic climate models were defined in the 1970s to be first applied to predict SSTA and thermocline variability (Hasselmann, 1976; Frankignoul and Hasselmann, 1977) and later addressing non-linearity problems (Majda et al., 1999). Moreover, Linear Inverse Modeling (Penland and Sardeshmukh, 1995) has been used in predicting variables such as tropical Atlantic SSTA (Penland and Matrosova, 1998) and the study of Atlantic Meridional Mode (Vimont, 2012). Statistical modeling with neural networks is also applied in climate prediction (Gardner and Dorling, 1998; Hsieh and Tang, 1998; Tang et al., 2000; Hsieh, 2001; Knutti et al., 2003; Baboo and Shereef, 2010; Shukla et al., 2011) with the potential to be a nonlinear method capable of ad-

GMDD
8, 3971–4018, 2015

S[4]CAST seasonal forecast model

R. Suárez-Moreno and B. Rodríguez-Fonseca

dressing the problems in atmospheric processes that are overlooked in other statistical methodologies (Tang et al., 2000; Hsieh, 2001).

A special mention goes to two linear statistical methods: Maximum Covariance Analysis (MCA) and Canonical Correlation Analysis (CCA). These methods have been widely used in seasonal climate forecasting, either to complement dynamical models or to be applied independently. In this way, Climate Predictability Tool (CPT) developed at International Research Institute for Climate and Society (IRI) allows user to apply multivariate linear regression techniques (e.g., CCA) to get their own predictions (Korecha and Barnston, 2007; Recalde-Coronel et al., 2014; Barnston and Tippet, 2014). In essence, these techniques serve to isolate co-variability coupled patterns between the time series of two variables (Bretherton et al., 1992). Based on the ability of the SSTA as predictor field, these methods were originally applied to analyze the predictability of variables such as ENSO (Barnston and Ropelewski, 1992), 500 mb height anomalies (Wallace et al., 1992) or global surface temperature and rainfall (Barnston and Smith, 1996). Nevertheless, there are works discussing the use of these methods, focusing on the differences between the two techniques (Cherry, 1996, 1997) and on the limitations in their applications (Newman and Sardeshmukh, 1995).

The co-variability patterns between SSTA themselves might fluctuate from one given study period to another, determining non-stationary behavior over time. In this way, teleconnections associated with El Niño or with the Tropical Atlantic are effective in some periods but not in others. In this way, Rodríguez-Fonseca et al. (2009) suggested how the interanual variability in the Atlantic could be used as predictor of Pacific ENSO after the 1970s, a theory that has been subsequently reinforced by further analysis (Martín-Rey et al., 2012, 2014; Polo et al., 2014). The non-stationarity in terms of predictability of rainfall has also been found for West African rainfall (Janicot et al., 1996; Fontaine et al., 1998; Mohino et al., 2011; Losada et al., 2012; Rodriguez-Fonseca et al., 2011, 2015); and Europe (López-Parages and Rodriguez-Fonseca, 2012; López-Parages et al., 2014). Thus, the existence of non-stationarities in the development of the statistical model is a key factor that has been taken into account.

GMDD
8, 3971–4018, 2015

The present paper describes a statistical model based on the predictive nature of SSTA treating the stationarity in the relationships between the predictor and predictand fields. Section 2 describes the theoretical framework including the statistical methodology and the significance of the statistical analysis. Section 3 is dedicated to S4CAST model description including the determination of stationary periods, hindcast and forecast calculations and validation. Section 4 describes a case study concerning the Sahelian rainfall predictability.

2 Theoretical framework

2.1 Statistical methodology

Maximum Covariance Analysis (MCA) is a broadly used statistical discriminant analysis methodology based on calculating principal directions of maximum covariance between two variables. This statistical analysis considers two fields, **Y** (predictor) and **Z** (predictand) (Bretherton et al., 1992; Cherry, 1997; Widmann, 2005) for applying the Singular Value Decomposition (SVD) to the cross-covariance matrix (**C**) in order to be maximized. SVD is an algebraical technique that diagonalizes non-squared matrices, as it can be the case of the matrices of the two fields to be maximized.

In the meteorological context, **C** is dimensioned in time (n_t) and space domains (n_Y and n_Z for **Y** and **Z** respectively), although the spatial domain can be more complex depending on the user requirements. SVD calculates linear combinations of the time series of **Y** and **Z**, named as expansion coefficients (hereinafter $\boldsymbol{U}$ and $\boldsymbol{V}$ for **Y** and **Z** respectively) that maximize **C**. The expansion coefficients are computed by diagonalization of **C**. As **C** is non-squared, diagonalization is first done to $\boldsymbol{A} = \boldsymbol{C}\boldsymbol{C}^T$ and then to $\boldsymbol{B} = \boldsymbol{C}^T\boldsymbol{C}$. The singular vectors $\boldsymbol{R}$ and $\boldsymbol{Q}$ are the resultant eigenvectors from each diagonalization, which are the spatial configurations of the co-variability modes. The associated loadings on time domain are the expansion coefficients $\boldsymbol{U}$ and $\boldsymbol{V}$. The eigenvalues are a measure of the variance percentage explained by each mode.

Mathematically, the time anomalies of both, **Z** and **Y** fields are calculated by removing the climatological seasonal cycle to the seasonal means.

$$\mathbf{Z}' = \mathbf{Z} - \overline{\mathbf{Z}} \tag{1}$$

$$\mathbf{Y}' = \mathbf{Y} - \overline{\mathbf{Y}} \tag{2}$$

Then, the cross-covariance matrix is calculated as:

$$\mathbf{C}_{Y'Z'} = \frac{\mathbf{Y}'\mathbf{Z}'^{T}}{(n_t - 1)} \tag{3}$$

MCA diagonalizes Eq. (3) by SVD methodology, obtaining the singular vectors $\boldsymbol{R}$ and $\boldsymbol{Q}$ from which the expansion coefficients are obtained according to the following expression:

$$\boldsymbol{U} = \boldsymbol{R}^{T}\mathbf{Y} \tag{4}$$

$$\boldsymbol{V} = \boldsymbol{Q}^{T}\mathbf{Z} \tag{5}$$

Using the eigenvectors, the percentage of explained covariance is calculated as

$$\mathrm{scf}_k = \frac{\lambda_k^2}{\sum_i^r \lambda_i^2}; \lambda_k = [\lambda_1, \lambda_2, \ldots, \lambda_n] \tag{6}$$

Where k is the eigenvalue for each k mode and r represents the number of modes taken into account for the analysis.

The expression from which an estimation of the predictand is obtained is a linear model as:

$$\hat{\mathbf{Z}} = \mathbf{\Phi}\mathbf{Y} \tag{7}$$

Where $\mathbf{\Phi}$ is the so-called regression coefficient and $\hat{\mathbf{Z}}$ denotes an estimation of the data to be predicted (hindcast).

Taking into account that $\mathbf{S}$ is the regression map of the field $\mathbf{Z}$ onto the direction of $\boldsymbol{U}$

$$\mathbf{S} = \boldsymbol{U}\mathbf{Z}^T \tag{8}$$

And assuming good prediction $\hat{\mathbf{Z}}$, it follows that

$$\mathbf{S} = \boldsymbol{U}\hat{\mathbf{Z}}^T \tag{9}$$

Introducing the equality $\left(\boldsymbol{U}\boldsymbol{U}^T\right)\left(\boldsymbol{U}\boldsymbol{U}^T\right)^{-1} = I$ and multiplying in Eq. (9) the following expression is obtained:

$$\left(\boldsymbol{U}\boldsymbol{U}^T\right)\left(\boldsymbol{U}\boldsymbol{U}^T\right)^{-1}\mathbf{S} = \boldsymbol{U}\hat{\mathbf{Z}}^T \tag{10}$$

Removing $\boldsymbol{U}$ from both terms

$$\hat{\mathbf{Z}} = \left[\boldsymbol{U}^T\left(\boldsymbol{U}\boldsymbol{U}^T\right)^{-1}\mathbf{S}\right]^T \tag{11}$$

Considering now the expression $\boldsymbol{U} = \mathbf{Y}^T\boldsymbol{R}$ it follows that

$$\hat{\mathbf{Z}} = \mathbf{Y}\boldsymbol{R}\left(\boldsymbol{U}\boldsymbol{U}^T\right)^{-1}\mathbf{S} \tag{12}$$

Comparing this expression with Eq. (7) and introducing Eq. (8) it can be concluded that

$$\mathbf{\Phi} = \boldsymbol{R}\left(\boldsymbol{U}\boldsymbol{U}^T\right)^{-1}\boldsymbol{U}\mathbf{Z}^T \tag{13}$$

Which is the regression coefficient to be calculated when defining the linear model from which the predictions and hindcasts will be obtained.

GMDD
8, 3971–4018, 2015
S4CAST seasonal forecast model
R. Suárez-Moreno and B. Rodríguez-Fonseca

2.2 Statistical field significance

There are many statistical tests to assess the robustness of a result. The S^{4}CAST uses a non-parametric test because, a priori, the model does not know the distribution of the predictand field. Thus, applying Monte Carlo testing assesses the robustness of the results and is used to validate the S^{4}CAST model skill. This method involves performing a large number ($N > 500$) of permutations from the original time series. Each permuted time series is used to perform the calculations again and compare the obtained results with the real values. Once this is done, the values obtained with the N permutations are taken to create a random distribution to finally determine the position of the real value within the distribution, which will indicate the statistical significance of the obtained value. This method has been described and used in several works (Livezey and Chen, 1987; Barnett, 1995; Maia et al., 2007). The user inputs the level of statistical significance at which the test is applied, being the most used 90 % (0.10), 95 % (0.05) and 99 % (0.01).

3 S^{4}CAST model

The first version of the model (S^{4}CAST v1.0) was developed as the main part of a cooperation project between the *Laboratoire de Physique de l'Atmosphère et de l'Océan Siméon Fongang* of the University Cheik Anta Diop (UCAD) in Dakar (Senegal) and the *Complutense* University of Madrid (UCM) and was limited to the study of the predictability of rainfall in West Africa from the SSTA in the tropical ocean basins. The second version (S^{4}CAST v2.0), described in this paper, has been expanded allowing the study of the predictability of any variable keeping a link with SSTA in any region worldwide. The code has been developed as a MATLAB® toolbox. The software requirements are variable and depend on user needs. The spatial resolution and size of data files used as inputs are directly proportional to memory requirements. The software generates an "out of memory" message whenever it requests a segment of memory from the operating system that is larger than what is currently available. The model software consists of three main modules (Fig. 1), each composed of a set of sub-modules whose operation is described below.

3.1 Model inputs

S^4CAST v2.0 has a direct execution mode. By simply typing *"S4cast"* in the command window, the user is prompted to enter a series of input parameters in a simple and intuitive way.

3.1.1 Loading databases

The model is ready to work with Network Common Data Form (NetCDF) data files. There are different conventions to set the attributes of the variables contained in NetCDF files. In this way, the data structure must conform as far as possible to the Cooperative Ocean/Atmosphere Research Service (COARDS) convention. Execution errors that may occur due to the selection of data files are easily corrected by minor modifications of data assimilation scripts. Data files can be easily introduced at the request of the user. Once downloaded from the website of a particular institution, the user inserts data files into the directory set by default (*S4CAST_v2.0/data_files)*.

3.1.2 Input parameters

In the first step, predictand and predictor data files are selected. In this way, the predictand field can be precipitation, SST, or any variable susceptible to be predicted from SSTA. The predictor is restricted to SST.

Once predictor and predictand fields are selected, the available common time period between them is analyzed and displayed so that the user is prompted to select the whole common period for analysis or other within it. The same temporal dimension in both fields is required in the statistical analysis to construct the cross-covariance matrix (see Sect. 2.1).

The next step is for selecting the n month forecast period in which the predictand is considered. The model allows a selection from one ($n = 1$) to four ($n = 4$) months. From the forecast period, the user determines a specific lead-time, relative to the predictor, from which medium-range (lead-time 0) or long-range (lead-time > 0) forecast can be performed. The temporal overlapping between the forecast period and the predictor is also available by defining the monthly lags between both fields from monthly lag 0 (synchronous) referred to the case in which the predictor and the predictand fields are taken at the same n month period, through partial overlap to eliminate the overlap (medium-range forecast). The forecast period must be determined by a previous study of the predictand over the prediction region (e.g., July-August-September when studying Sahelian rainfall variability). Monthly lags indicating forecast times (lead-times) are user selectable. To illustrate the above, if forecast period corresponds to rainy season in West Africa (July-August-September; JAS), the synchronous option will consider the predictor in JAS, while partially overlapping occurs when the predictor is taken for June-to-August (JJA) and May-to-July (MJJ). A forecast time equal to zero (lead-time equal to zero) is referred to the period from April–June (AMJ). The lead-times (lags) depend on the forecast period so that the model requires the input of this parameter for establishing the data concerning the predictor. Considering the above options, the user can select a sequence of successive monthly lags or only one. Following the previous example, considering JAS as the forecast period, lead time 0 will be AMJ, lead time 1 will be MAM, lead time 2 will be FMA and so on, without overlapping JAS season of the previous year. Thus, the user can select any 3 month isolated period from JAS (synchronous) to OND. Next, the spatial domains of both predictor and predictand fields are selected from its latitudinal and longitudinal values.

Later, there is the possibility of applying a filter to the time series of predictor and predictand fields. The current version uses a Butterworth filter, either as high-pass or low-pass filter, which are frequently used in climate-related studies (e.g., Roe and Steig, 2004; Enfield and Cid-Serrano, 2006; Mokhov and Smirnov, 2006; Ault and George, 2012; Schurer and Hegerl, 2013). This filter allows the user to isolate the frequencies at which the variability operates, which can have different sources of predictability. In this way, the user selects the cutoff frequency, following the expression $2\mathrm{d}t/T$, being $\mathrm{d}t$ the sampling interval and T the period to be filtered both in the same units of time. If no filter is applied, the raw data is used. There are plenty of filters that could be applied and future versions of the model will include different possibilities.

The statistical methodology is applied first considering the longer forecast time defined by the selected lead-time and successively adding information for all other lead-times up to the present. So, continuing with the example above, if selected lead-times from 0 to 3, the first predictor matrix is made considering the 3 months lead-time period (JFM). After, the 2 months lead-time period is added (JFM + FMA). Next, up to the period 1 month delayed (JFM + FMA + MAM), and finally the case up to the period with a lead-time equal to zero (JFM + FMA + MAM + AMJ). Previous example is illustrated in Fig. 2.

Once the matrices are determined, the statistical methodology is selected. Up to now, the model applies the MCA discriminant analysis technique, although other statistical methodologies will be included in future releases, including CCA or non-linear methods as neural network and Bayesian methodologies. As indicated in the previous section, MCA determines a new vector base in which the relations between the variables are maximized. Thus, it is important to choose a number of modes (principal directions) to be considered in the computations, selecting either a single mode or a set of them, always consecutive. The analysis of stationarity is performed for a single mode selection. For multi-mode selection, the whole time series will be considered.

The statistical field significance level is set for the first time to assess the analysis of stationarity. Thus, the model runs for the entire period and for those periods for which the relationships are considered stationary within it. This is internally established by applying the method explained later in the Sect. 3.2.1.

3.1.3 Data preprocessing

From selected data files and input parameters previously defined, preprocessing of data is performed so that the data are prepared for implementing statistical methodology.

3.2 Statistical tools

At this point the statistical procedure described in the methodology is applied considering different periods based on the analysis of stationarity described below.

3.2.1 Analysis of stationarity

To evaluate how much the time series of the expansion coefficients of the predictor (**Y**) and the predictand (**Z**) fields are related to each other, the model calculates the correlation coefficients between the expansion coefficients indicated in Eqs. (4) and (5) for the selected kth mode along the record. In this way, stationary relationships between the predictor (**Y**) and the predictand (**Z**) fields are established by applying a 21 years moving correlation windows analysis between the leading expansion coefficients of both fields obtained from the discriminant analysis method using the whole record in accordance with the evolution of the correlation coefficient. To do this, three types of 21 years moving correlation windows are selectable: "delayed" to correlate one year and the 20 previous years; "centered" to correlate one year, the 10 previous years and the 10 next years; or "advanced" to correlate one year and the 20 next years.

From previous analysis, three different periods are analyzed depending on the stationarity of the predictability: use the significant correlation period (hereafter SC) for which the expansion coefficients are significantly correlated; use no significant correlation period (hereafter NSC), and work with the entire period (hereafter EP). The model performs all calculations for each period separately and, from them, the simulated maps (hindcasts) of the predictand for each year are calculated by applying cross-validation.

3.2.2 Model validation

Cross-validation is used in climate forecasting as part of statistical models when assessing forecast skill (Michaelsen, 1987; Barnston and Van den Dool, 1993; Elsner and Schmertmann, 1994). This method is intended as a model validation technique in which the data for the predictor and the predictand for a given time step is removed from the analysis to make an estimate of it with the rest of data, comparing the simulated value with the removed one. In this way, a cross-validated hindcast is obtained. In the S^4CAST model, the one-leave-out method is applied as described by (Dayan et al., 2013). From the comparison between the predicted value and the original one, the skill of the model can be inferred using different skill-scores. S^4CAST considers the Pearson correlation coefficients and the root mean square error (RMSE) although other scores will be introduced in future versions.

3.3 Model outputs

Modes of co-variability are related to spatial patterns of different variables that co-vary over time, and thus, are linked to each other. In the case of MCA, the covariance matrix is computed and the SVD method is applied to provide a new basis of eigenvectors for the predictor and predictand fields which covariance is maximized. The obtained singular vectors describe spatial patterns of anomalies in each of the variables that tend to be related to each other. Regression and correlation maps and corresponding expansion coefficients determine each mode of co-variability for the predictor and predictand fields. The expansion coefficients indicate the weight of these patterns in each of the time steps. Thus, regression and correlation co-variability maps can be represented. This is done with the original anomalous matrix, highlighting those grid points whose time series are highly correlated with the obtained expansion coefficients, show-

GMDD
8, 3971–4018, 2015

ing large co-variability and determining the key regions of prediction. To represent it, regression and correlation maps are calculated to analyze the coupling between variables and to understand the physical mechanisms involved in the link.

On the other hand, the time series of the expansion coefficients determine the scores of the regression and correlation maps at each time along the study period. The model represent the expansion coefficients used to calculate the regression coefficients. Thus, those years in which the expansion coefficients for the predictor and the predictand are highly correlated will coincide with years in which we can expect a better estimation.

In the current version of the model, the root mean square error (RMSE) and the Pearson correlation coefficients skill scores have been included. These techniques are applied to compare the observed and simulated maps (hindcasts) of the predictand field obtaining correlation and RMSE maps and time series. On the one hand, maps are obtained calculating for each grid point the skill scores between the hindcast and the observed maps. On the other hand, time series are obtained for each time by applying correlation and RMSE between the area average of the observed and estimated maps. Some comments on these techniques are addressed by Barnston (1992). The S^4CAST model generates the hindcast within the EP, SC and NSC periods separately from applying the one-leave-out method (Dayan et al., 2013) and then the statistical methodology.

4 Case study: Sahelian rainfall

The WAM is characterized by a strongly seasonal rainfall regime that mainly occurs from July to September related to the semi-annual shift of the Intertropical Convergence Zone (ITCZ) together with the presence of a strong thermal gradient between the Sahara and the ocean in the Gulf of Guinea. The interannual fluctuations in seasonal rainfall are due to various causes, being the changes in global SST the main driver of WAM variability (Rodríguez-Fonseca et al., 2015).

S^4CAST model is conceived as a statistical tool to forecast variables that strongly covariate with SSTA variability in remote and nearby locations to a particular region of study. Up to now, the model has been applied to study the predictability of rainfall considering the non-stationary influence of the different oceanic predictors along the historical record. In this section the model has been validated through the study of the seasonal rainfall predictability in the Western Sahel from SSTA in the tropical Atlantic sector. This choice is motivated by two main reasons: on the one hand, SST in the tropical Atlantic is well known to strongly influence the dynamics of the ITCZ (Fontaine et al., 1998) which in turn determines the subsequent WAM. Nevertheless, dynamical models do not reproduce the influence of SST on the ITCZ (Lin, 2007; Richter and Xie, 2008; Doi et al., 2012; Tonniazzo and Woolnough, 2013) becoming the statistical prediction an alternative way to predict WAM variability. The second reason is related to the non-stationary influence of the tropical Atlantic on Sahelian rainfall reported in some studies (Janicot et al., 1996, 1998; Ward, 1998; Rodríguez-Fonseca et al., 2011; Mohino et al., 2011; Losada et al., 2012).

Two simulations were launched, both with the same inputs except for the predictors, which are selected in different seasons (explained before). The predictand field corresponds to precipitation from GPCC Full Data Reanalysis monthly means of precipitation appended with GPCC monitoring dataset from 2011 onwards with a resolution of $1.0^\circ \times 1.0^\circ$ covering the period from January 1901 to November 2014 (Rudolf et al., 2010; Becker et al., 2013; Schneider et al., 2014; http://gpcc.dwd.de). The predictor field corresponds to NOAA Extended Reconstructed SST (ERSST) V3b monthly means of SST with a resolution of $2.0^\circ \times 2.0^\circ$ spanning the period from January 1854 to January 2015 (Smith and Reynolds, 2003, 2004; Smith et al., 2008; http://www.esrl.noaa.gov/psd/data/gridded/data.noaa.ersst.html). The forecast period consists of July to September (JAS) season, computing seasonal anomalous rainfall in the Sahelian domain (18.5–10.5° W; 12.5–17.5° N) as predictand field with no frequency filter applied. The predictor spatial domain corresponds to southern subtropical and equatorial Atlantic band (60° W–20° E; 20° S–4° N).

GMDD
8, 3971–4018, 2015

S^4CAST seasonal forecast model

R. Suárez-Moreno and B. Rodríguez-Fonseca

A high pass filter with cutoff frequency set to 7 years has been applied to the predictor time series in order to analyze the influence of SSTA interannual variability, which includes leading oceanic interannual variability modes such as the Atlantic equatorial mode (AEM) (Polo et al., 2008) or the South Atlantic Ocean dipole (SAOD) (Nnamchi et al., 2011) and removes decadal and multidecadal variability.

For seasons where the predictor is taken, on the one hand, multiple selection has been selected, which refers to the synchronous season (July to September; JAS) in addition to monthly overlaps (June to August JJA and May to July MJJ) regarding the predictand field. In this case the predictor is formed by a set of matrices as shown in Fig. 2. This selection is hereinafter referred as synchronous. On the other hand, lead-time zero was selected (April to June; AMJ), allowing a real prediction. Table 1 lists the case studies depending on the stationary periods and the selection of the predictor seasons. The results are shown for the synchronous selection (MJJ + JJA + JAS) corresponding to SL1. When SL0 is considered, the season with a lead-time set to zero (AMJ) is taken for predictor, so that the temporal overlap between the predictor and the predictand is avoided.

The analysis method corresponds to MCA, for which the leading mode of co-variability ($k = 1$) was selected. Periods with stationary predictability (SC and NSC) are established by the method explained in Sect. 3.2.1 between the predictor and predictand expansion coefficients for the entire period (EP). Two correlation curves are shown for SL0 and SL1 selections (Fig. 3). These curves reflect the stationary periods (SC and NSC) within EP period from 1902 to 2013 depending on the predictor selections (see Table 1). The curve corresponding to SL0 shows the SC period related to years from 1933 to 1971, while SL1 exhibit a SC period related to years from 1932 to 1984. The remaining years for each selection are taken to analyze the predictability for the NSC periods. When the statistical analysis is applied over the entire period we refer to non-stationary influence (EP-SL0 and EP-SL1), assuming changes in predictability. Stationary cases are related to the analysis applied to SC (SC-SL0 and SC-SL1) and NSC (NSC-SL0 and NSC-SL1) periods, for which the model produces a series of estimations (hindcasts) separately. The statistical significance in all the calculations has been set to 90 %.

Figures 4–6 show regression maps associated with the leading mode of co-variability for each period (SC, NSC, EP) and predictor (SL0, SL1). For SC-SL0 case study, the leading mode explains 53 % of co-variability while the percentage increases to 58 % for SC-SL1. A quasi isolated signal over tropical Atlantic (Fig. 4) is observed, being stronger the magnitude of SSTA and appearing a signal of opposite sign in the coast of Senegal when tackling SC-SL0 case. This co-variability pattern, for its positive phase, exhibits a cooling over tropical Atlantic associated with a rainfall dipole over West Africa with negative anomalies in the region of the Gulf of Guinea and opposite in the Sahel. The opposite co-variability pattern takes place under negative scores of the expansion coefficient. These results are in agreement with those found in the last decades of the 20th century by several authors who have discussed the role of the tropical Atlantic SST as a dominant factor in the WAM variability at interannual and seasonal time scales (Janowiak, 1988; Janicot, 1992; Fontaine and Janicot, 1996). Also, Losada et al. (2010b) found how the response to an isolated positive equatorial Atlantic Niño event is a dipolar rainfall pattern in which the decrease of rainfall in Sahel is related to the increase of rainfall in Guinea (as in Fig. 4). Mohino et al. (2011) and Rodríguez-Fonseca et al. (2011) have found in the observations how this dipolar behavior takes place for some particular decades coinciding with the SC periods, confirming in this way the correct determination of the leading co-variability mode by the model.

When considering the EP period (Fig. 5) the leading mode explains 44 and 41 % of co-variability between SSTA and rainfall for EP-SL0 and EP-SL1 respectively. As in the case of considering the SC period (Fig. 4), a cooling over tropical south Atlantic is associated with a rainfall dipole over West Africa with positive anomalies over the Sahel and negative in the Gulf of Guinea. Nevertheless the anomalous rainfall signal is less intense in both cases (EP-SL0 and EP-SL1) when compared to SC. Opposite sign anomalies are observed over the tropical North Pacific and around the coast of California about 20° N, specially when EP-SL0 is considered for predictor.

Regarding the NSC period (Fig. 6), the leading mode explains 30 % of co-variability for NSC-SL0 case and 22 % for NSC-SL1. Both cases relate a cooling in the tropical Atlantic with negative rainfall anomalies in the Gulf of Guinea (vice versa for a warming), and no opposite signal over the Sahel. This result agrees with former studies in which the disappearance of the rainfall dipole associated to interannual equatorial Atlantic variability was attributed to the remote influence of other basins (Rodríguez-Fonseca et al., 2011; Losada et al., 2012). The global SSTA regression map shows a significant cooling in the tropical Pacific, suggesting its influence when NSC periods are considered. A similar tropical SSTA pattern in which opposite temperature anomalies appears in the equatorial Atlantic and Pacific in summer has been documented to occur in the decades within the NSC period (Rodríguez-Fonseca et al., 2009; Martin-Rey et al., 2012, 2014), confirming the correct determination of the leading co-variability mode by the model.

The results presented above support the existence of a non-stationary behavior of the teleconnections between SSTA variability and rainfall associated with WAM which has been referenced in the previously mentioned works. Several authors have addressed the dipolar anomalous rainfall pattern as a response of an isolated tropical Atlantic warming (cooling) (Rodríguez-Fonseca et al., 2011; Losada et al., 2010a, b; Mohino et al., 2011) always restricted to the period 1957–1978 in the observations. The uniform rainfall signal over the whole West Africa, with negative anomalies related to a cooling over tropical Atlantic and an opposite sign pattern over tropical Pacific is only observed for the period from 1979 in advance. These results agree with Losada et al. (2012), who focused on non-stationary influences of tropical global SST in WAM variability, finding an Indian and Pacific correlated signal from 1970s in addition to the isolated Atlantic influence prior to that period which is accompanied by the rainfall dipole over West Africa. Recently, Diatta and Fink (2014) have documented similar non-stationary relationships.

By comparing the hindcasts and observations in each grid point and time, validation is computed. To do this, the Pearson correlation coefficient has been used, so that the

GMDD
8, 3971–4018, 2015

S^4CAST seasonal forecast model

R. Suárez-Moreno and B. Rodríguez-Fonseca

associated skill of the model to reproduce the rainfall is shown in Fig. 7 in terms of correlation maps over the study region under each of the considered periods (SC, NSC, EP). As a first result, a qualitative improvement is observed when considering the SC periods instead of the whole period (EP). This result points to a better spatial distribution of the significant values for particular decades in which the signal extends to a larger spatial domain, mainly in the southwestern region. In order to analyze the performance of the simulation for each particular year, the correlation between observed and predicted maps at each time step is calculated and shown in Fig. 7. Since it has only been considered the leading mode of co-variability, the time series of validation between observed and simulated rainfall should evolve following the absolute values of the expansion coefficients. Thus, when the expansion coefficient (U) of the predictor (SST) shows high scores in the leading mode, good hindcasts are generally obtained.

The rest of cases (NSC periods) show bad skill in terms of negative correlation (Fig. 8), indicating how the leading mode of co-variability when considering the whole time series is not useful for predicting rainfall in particular decades as those in NSC.

To complement the results obtained by the model, the data matrix for the predictor (Y) and the predictand (Z) fields have been used in the Climate Predictability Tool (CPT) developed at IRI. Thus, CCA method has been used, providing the results for the leading mode of co-variability (Fig. 11) considering the whole study period (EP-SL0).

The leading mode by using CPT relates positive values of the SST over tropical Atlantic with a rainfall decrease over the study region and vice versa, supporting the results found in this study with the S^{4}CAST model. Nevertheless, the obtained results related to the skill of the CPT to reproduce rainfall variability (Fig. 10), show negative values by using Pearson correlation coefficients, but lower than those obtained with the S^{4}CAST model. The results of CPT are not so good as those using S^{4}CAST. Thus, the inclusion of a stationarity analysis to discriminate periods with changes in predictability is crucial to improve the forecast skill.

5 Discussion and conclusions

This paper introduces the S^4CAST v2.0 model, developed at the Department of Geophysics and Meteorology, in the Faculty of Physics of the Universidad Complutense de Madrid (UCM). The model was created from the first version (S^4CAST v1.0), developed as part of a cooperation project with the Laboratoire de Physique de l'Atmosphère et de l'Océan Siméon Fongang (LPAOSF) of the Université Cheikh Anta Diop (UCAD) of Dakar in Senegal.

The model is focused on the study of the predictability of climate-related variables based on the predictive nature of the SST. Such variables can be either SST (Rasmusson and Carpenter, 1982; Latif and Barnett, 1995; Harrison and Larkin, 1998; Klein et al., 1999; Trenberth et al., 2002) and rainfall (Janicot et al., 2001; Rowell, 2001, 2003; Giannini et al., 2003; Chung and Ramathan, 2006; Polo et al., 2008; Joly and Voldoire, 2009; Lu, 2009; Gaetani et al., 2010; Fontaine et al., 2011; Nnamchi and Li, 2011); but also other variables. There are studies that have focused on the role of the tropical Pacific on vegetation, crop yields and the economic consequences resulting from these impacts (Hansen et al., 1998, 2001; Adams et al., 1999; Legler et al., 1999; Li and Kafatos, 2000; Naylor et al., 2001; Tao et al., 2004; Deng et al., 2010; Phillips et al., 1998; Verdin et al., 1999; Podestá et al., 1999; Travasso et al., 2009). Regarding human health, tropical SST patterns have been widely linked to the development and propagation of diseases (Linthicum et al., 2010), where ENSO-related variability plays a crucial role mainly affecting tropical and subtropical regions around the world (Kovats, 2000; Patz, 2002; Kovats et al., 2003; Patz et al., 2005; McMichael et al., 2006). Whatever the predictand, previous analysis of the SST influence is necessary in order to establish an association between such variables and the SST variability considered as the predictor field.

Concerning the association between two variables along time, the concept of stationarity is raised as one of the motivating factors in creating the S^4CAST model. The stationarity refers to changes in the co-variability patterns between the predictor and the predictand fields along a given sequence of decades, so that it can be kept invariant (stationary) or changing (non-stationary). This concept has been addressed by different authors (Janicot et al., 1996; Fontaine et al., 1998; Rodríguez-Fonseca et al., 2009, 2011; Mohino et al., 2011; Martín-Rey et al., 2012; Losada et al., 2012) and becomes the main novelty and contribution introduced by S^{4}CAST as a key factor to consider in seasonal forecasting provided by current prediction models, either dynamical or statistical. Thus, S^{4}CAST model is an alternative to enhance and complement the estimates made by dynamical models, which have a number of systematic errors to adequately reproduce the tropical climate variability (Biasutti et al., 2006; Richter and Xie, 2008; Wahl et al., 2011; Doi et al., 2012; Richter et al., 2012; Bellenguer et al., 2013; Brown et al., 2013; Li and Xie, 2013; Toniazzo and Woolnough, 2013; Vanniere et al., 2013; Xue et al., 2013). For the time being, the S^{4}CAST model cannot be applied for strict operational forecasts, although its application in determining stationary relationships between two fields and their co-variability patterns can be crucial for improving the estimates provided by the operating prediction models currently used.

In the application shown in this paper we have focused in the results from MCA. This statistical methodology, along with Canonical Correlation Analysis (CCA), have been widely used in studies of predictability during the last decades (Barnston and Ropelewski, 1992; Bretherton et al., 1992; Wallace et al., 1992; Barnston and Smith, 1996; Fontaine et al., 1999; Korecha and Barnston, 2007; Barnston and Tippet, 2014; Recalde-Coronel et al., 2014). Integration of the methodology and intuitive use through a user interface are some of the main advantages of the S^{4}CAST model, allowing the selection of a big number of inputs. Future releases of the model will include other methodologies that are currently being introduced and tested.

When conducting a pooling of the performance from models, a conclusion can be posed. On the one hand, dynamical models produce an underestimation of seasonal climate forecasts, partly because the difficulty of reproducing the influence of SST on atmospheric dynamics, and on the other hand, the chaotic behavior of the atmosphere is markedly exaggerated in these models. In contrast, statistical models, despite being an useful and effective supplement, mostly they are unable to reproduce the non-linearity in the ocean–atmosphere system, exceptions include neural networks and Bayesian methods. Attempts to implement new statistical models constitute a fundamental contribution aimed to enhance and complement the dynamical models. Anyway, statistical models have evolved linked to dynamical models, either as an alternative or within them as a hybrid model.

The application of moving correlation windows between expansion coefficients obtained from MCA analysis results in three periods of stationarity: entire period (EP), significant correlation period (SC) and no-significant correlation period (NSC). For the case in which non-stationarity is considered we refer to EP period, assuming changes in co-variability patterns. Stationarity is referred to SC and NSC periods. These periods may slightly vary depending on the type of moving correlation windows: advanced, centered or delayed. Stationary analysis to determine the three different work periods (SC, NSC, EP) is limited to the selection of a single mode of co-variability using MCA analysis. When selecting a set of modes, stationarity analysis is not applied so that simulations are only developed for EP period, whereby the whole time series is considered for both the predictor and predictand fields. Future releases of S^{4}CAST will include new techniques in order to assess stationarity periods, being hierarchical Bayesian methods one of the next steps to improve the model.

Three conditions may enhance the degree of confidence in a given predictor. The first has to do with the selection of moving correlation windows (see Sect. 3.1.2) used to determine the working scenarios (SC, NSC, EP). Delayed moving correlation windows can help in this task. Thus, if correlation coefficients between the expansion coefficients (U and V) exhibit significant values for the present year and the previous 21 study years, greater confidence is assumed for the predictor. The second condition is determined by the value of the expansion coefficient (U) for the current year so that the higher its value, the better the forecast. The last condition has to do with the percentage of variance explained by the selected co-variability mode, the higher its value, the better the forecast. Nevertheless, despite previous conditions, the influence of other remote

GMDD
8, 3971–4018, 2015

and nearby oceanic predictors must be considered in order to provide a full and reliable predictability study.

So far, the data files used as predictor and predictand fields correspond to observations and reanalysis from several institutions. The use of new data files is simple and can be performed according to user needs. The upgrade of data files from respective websites must be checked periodically to strengthen the results. In addition, it is also advisable to launch the same simulations using different data files in order to compare the results and assess the robustness of the forecast. The results shown in this work for different selections (SC-SL0, SC-SL1, NSC-SL0, NSC-SL1, EP-SL0, EP-SL1) have been verified by following these criteria.

Originally, the model was created to tackle the study of the predictability of anomalous rainfall associated with WAM, which co-varies in a different way with the tropical band of Atlantic and Pacific ocean basins, being an indicator of non-stationarity (Losada et al., 2012). The case study developed in this work corresponds to the predictability of Sahelian rainfall in the prominent season (JAS) from SSTA in the tropical Atlantic, serving as a benchmark for the model. The transition between SC and NSC periods, around the 1970s, has served as the starting point of many studies focusing on the influence of global SSTA before and after that period (Mohino et al., 2011; Rodríguez-Fonseca et al., 2011, 2015; Losada et al., 2012) while being one of the motivations to create S^{4}CAST.

The results obtained by using the CPT tool, demonstrate the ability of S^{4}CAST to improve the predictability of climate variability associated with the WAM and put forward the consideration of non-stationarity in the co-variability patterns and therefore in climatic teleconnections. Thus, it is important to determine the multidecadal modulator of the interannual variability in order to know which predictor is the one affecting in particular periods and regions (Rodríguez-Fonseca et al., 2015).

Code availability

The model consists of a software package organized in folders containing libraries, functions and scripts developed as a MATLAB® toolbox from version R2010b onwards. Two of the folders, named as *mexcdf* and *netcdf_toolbox*, corresponds to libraries needed for working with NetCDF files and have been downloaded from www.mexcdf.sourceforge.net and built-in into the model. The file containing the model core with the executable code is named *S4core*. Once the toolbox has been added to the MATLAB® path and by simply typing *"S4cast"* in the command window, the user is prompted to enter a number of input parameters required to launch a simulation. Additionally, the software package *S4plot* dedicated to plot figures has been added so that the user can use this software by typing *"figures"* in the command window once the simulation has ended and the output data are loaded. The code is Open Access and can be downloaded from the Zenodo repository (DOI 10.5281/zenodo.15985) in the URL https://zenodo.org/record/15985. Along with the code, there is a text file containing inputs leading to the results presented in this paper for SL0 (*sahelian_rainfall_inputs_SL0.txt*) and SL1 (*sahelian_rainfall_inputs_SL1.txt*) case studies. Note that figures presented in this work have been further improved manually. To facilitate implementation of the model leading to the results shown in this paper, used data files that have been previously defined in Sect. 4, are included in the directories */S4CAST_v2.0/data_files/predictand* and */S4CAST_v2.0/data_files/predictor*. The code has been thoroughly analyzed by using several data files and input parameters. However, the emergence of software bugs is not ruled out, being mostly associated with problems to adapt and use NetCDF files. To solve these hypothetical code bugs, please do not hesitate to contact authors.

Acknowledgements. The research leading to these results received funding from the EU FP7/2007-2013 under grant agreement no. 603521, Spanish national project MINECO (CGL2012-38923-C02-01) and the VR: 101/11 project from the VIII UCM Call for Cooperation and Development projects. We also appreciate the work done by SOURCEFORGE.NET®

staff in creating NetCDF libraries for MATLAB®. And of course, thanks also to the reviewers, editors and their advice and/or criticism.

References

Adams, R. M., Chen, C. C., McCarl, B. A., and Weiher, R. F.: The economic consequences of ENSO events for agriculture, Clim. Res., 13, 165–172, 1999.

Ashok, K., Guan, Z., and Yamagata, T.: Impact of the Indian Ocean dipole on the relationship between the Indian monsoon rainfall and ENSO, Geophys. Res. Lett., 28, 4499–4502, 2001.

Ault, T. R., Cole, J. E., and St George, S.: The amplitude of decadal to multidecadal variability in precipitation simulated by state-of-the-art climate models, Geophys. Res. Lett., 39, L21705, doi:10.1029/2012GL053424, 2012.

Baboo, S. S. and Shereef, I. K.: An efficient weather forecasting system using artificial neural network, International Journal of Environmental Science and Development, 1, 321–326, 2010.

Barnett, T. P.: Monte Carlo climate forecasting, J. Climate, 8, 1005–1022, 1995.

Barnett, T. P. and Preisendorfer, R.: Origins and levels of monthly and seasonal forecast skill for United States surface air temperatures determined by canonical correlation analysis, Mon. Weather Rev., 115, 1825–1850, 1987.

Barnett, T. P., Graham, N., Pazan, S., White, W., Latif, M., and Flügel, M.: ENSO and ENSO-related predictability, Part I: Prediction of equatorial Pacific sea surface temperature with a hybrid coupled ocean–atmosphere model, J. Climate, 6, 1545–1566, 1993.

Barnston, A. G.: Correspondence among the correlation, RMSE, and Heidke forecast verification measures; refinement of the Heidke score, Weather Forecast., 7, 699–709, 1992.

Barnston, A. G. and Ropelewski, C. F.: Prediction of ENSO episodes using canonical correlation analysis, J. Climate, 5, 1316–1345, 1992.

Barnston, A. G. and Smith, T. M.: Specification and prediction of global surface temperature and precipitation from global SST using CCA, J. Climate, 9, 2660–2697, 1996.

Barnston, A. G. and Tippett, M. K.: Climate information, outlooks, and understanding – where does the IRI stand?, Earth Perspectives, 1, 1–17, 2014.

Barnston, A. G. and van den Dool, H. M.: A degeneracy in cross-validated skill in regression-based forecasts, J. Climate, 6, 963–977, 1993.

GMDD
8, 3971–4018, 2015

Barnston, A. G., van den Dool, H. M., Rodenhuis, D. R., Ropelewski, C. R., Kousky, V. E., O'Lenic, E. A., and Leetmaa, A.: Long-lead seasonal forecasts – where do we stand?, B. Am. Meteorol. Soc., 75, 2097–2114, 1994.
Barnston, A. G., He, Y., and Glantz, M. H.: Predictive skill of statistical and dynamical climate models in SST forecasts during the 1997–98 El Niño episode and the 1998 La Niña onset, B. Am. Meteorol. Soc., 80, 217–243, 1999.
Becker, A., Finger, P., Meyer-Christoffer, A., Rudolf, B., Schamm, K., Schneider, U., and Ziese, M.: A description of the global land-surface precipitation data products of the Global Precipitation Climatology Centre with sample applications including centennial (trend) analysis from 1901–present, Earth Syst. Sci. Data, 5, 71–99, doi:10.5194/essd-5-71-2013, 2013.
Bellenger, H., Guilyardi, E., Leloup, J., Lengaigne, M., and Vialard, J.: ENSO representation in climate and models: from CMIP3 to CMIP5, Clim. Dynam., 42, 1999–2018, 2013.
Biasutti, M., Sobel, A. H., and Kushnir, Y.: AGCM precipitation biases in the tropical Atlantic, J. Climate, 19, 935–958, 2006.
Biasutti, M., Held, I. M., Sobel, A. H., and Giannini, A.: SST forcings and Sahel rainfall variability in simulations of the twentieth and twenty-first centuries, J. Climate, 21, 3471–3486, 2008.
Bjerknes, J.: Atmospheric teleconnections from the equatorial Pacific 1, Mon. Weather Rev., 97, 163–172, 1969.
Bretherton, C. S., Smith, C., and Wallace, J. M.: An intercomparison of methods for finding coupled patterns in climate data, J. Climate, 5, 541–560, 1992.
Brown, J. N., Gupta, A. S., Brown, J. R., Muir, L. C., Risbey, J. S., Whetton, P., and Wijffels, S. E.: Implications of CMIP3 model biases and uncertainties for climate projections in the western tropical Pacific, Climatic Change, 119, 147–161, 2013.
Bulić, I. H. and Kucharski, F.: Delayed ENSO impact on spring precipitation over North/Atlantic European region, Clim. Dynam., 38, 2593–2612, 2012.
Cane, M. A., Zebiak, S. E., and Dolan, S. C.: Experimental forecasts of EL Nino, Nature, 321, 827–832, 1986.
Chang, P., Fang, Y., Saravanan, R., Ji, L., and Seidel, H.: The cause of the fragile relationship between the Pacific El Nino and the Atlantic Nino, Nature, 443, 324–328, 2006.
Cherry, S.: Singular value decomposition analysis and canonical correlation analysis, J. Climate, 9, 2003–2009, 1996.
Cherry, S.: Some comments on singular value decomposition analysis, J. Climate, 10, 1759–1761, 1997.

GMDD
8, 3971–4018, 2015
S4CAST seasonal forecast model
R. Suárez-Moreno and B. Rodríguez-Fonseca

Chung, C. E. and Ramanathan, V.: Weakening of North Indian SST gradients and the monsoon rainfall in India and the Sahel, J. Climate, 19, 2036–2045, 2006.
Coelho, C. A. S., Stephenson, D. B., Balmaseda, M., Doblas-Reyes, F. J., and van Oldenborgh, G. J.: Toward an integrated seasonal forecasting system for South America, J. Climate, 19, 3704–3721, 2006.
Dayan, H., Vialard, J., Izumo, T., and Lengaigne, M.: Does sea surface temperature outside the tropical Pacific contribute to enhanced ENSO predictability?, Clim. Dynam., 43, 1311–1325, 2014.
Deng, X., Huang, J., Qiao, F., Naylor, R. L., Falcon, W. P., Burke, M., and Battisti, D.: Impacts of El Niño–Southern Oscillation events on China's rice production, J. Geogr. Sci., 20, 3–16, 2010.
Diatta, S. and Fink, A. H.: Statistical relationship between remote climate indices and West African monsoon variability, Int. J. Climatol., 34, 3348–3367, doi:10.1002/joc.3912, 2014.
Ding, H., Keenlyside, N. S., and Latif, M.: Impact of the equatorial Atlantic on the El Nino southern oscillation, Clim. Dynam., 38, 1965–1972, 2012.
Doi, T., Vecchi, G. A., Rosati, A. J., and Delworth, T. L.: Biases in the Atlantic ITCZ in seasonal-interannual variations for a coarse-and a high-resolution coupled climate model, J. Climate, 25, 5494–5511, 2012.
Drosdowsky, W. and Chambers, L. E.: Near-global sea surface temperature anomalies as predictors of Australian seasonal rainfall, J. Climate, 14, 1677–1687, 2001.
Elsner, J. B. and Schmertmann, C. P.: Assessing forecast skill through cross validation, Weather Forecast., 9, 619–624, 1994.
Enfield, D. B. and Cid-Serrano, L.: Projecting the risk of future climate shifts, Int. J. Climatol., 26, 885–895, 2006.
Folland, C. K., Palmer, T. N., and Parker, D. E.: Sahel rainfall and worldwide sea temperatures, 1901–85, Nature, 320, 602–607, 1986.
Fontaine, B. and Janicot, S.: Sea surface temperature fields associated with West African rainfall anomaly types, J. Climate, 9, 2935–2940, 1996.
Fontaine, B., Trzaska, S., and Janicot, S.: Evolution of the relationship between near global and Atlantic SST modes and the rainy season in West Africa: statistical analyses and sensitivity experiments, Clim. Dynam., 14, 353–368, 1998.

Fontaine, B., Philippon, N., and Camberlin, P.: An improvement of June–September rainfall forecasting in the Sahel based upon region April–May moist static energy content (1968–1997), Geophys. Res. Lett., 26, 2041–2044, 1999.

Fontaine, B., Monerie, P. A., Gaetani, M., and Roucou, P.: Climate adjustments over the African-Indian monsoon regions accompanying Mediterranean Sea thermal variability, J. Geophys. Res.-Atmos., 116, D23122, doi:10.1029/2011JD016273, 2011.

Frankignoul, C. and Hasselmann, K.: Stochastic climate models, part II application to sea-surface temperature anomalies and thermocline variability, Tellus, 29, 289–305, 1977.

Gaetani, M., Fontaine, B., Roucou, P., and Baldi, M.: Influence of the Mediterranean Sea on the West African monsoon: intraseasonal variability in numerical simulations, J. Geophys. Res.-Atmos., 115, D24115, doi:10.1029/2010JD014436, 2010.

Gardner, M. W. and Dorling, S. R.: Artificial neural networks (the multilayer perceptron) – a review of applications in the atmospheric sciences, Atmos. Environ., 32, 2627–2636, 1998.

Garric, G., Douville, H., and Déqué, M.: Prospects for improved seasonal predictions of monsoon precipitation over Sahel, Int. J. Climatol., 22, 331–345, 2002.

Giannini, A., Chiang, J. C., Cane, M. A., Kushnir, Y., and Seager, R.: The ENSO teleconnection to the tropical Atlantic Ocean: contributions of the remote and local SSTs to rainfall variability in the tropical Americas*, J. Climate, 14, 4530–4544, 2001.

Giannini, A., Saravanan, R., and Chang, P.: Oceanic forcing of Sahel rainfall on interannual to interdecadal time scales, Science, 302, 1027–1030, 2003.

Gill, A.: Some simple solutions for heat-induced tropical circulation, Q. J. Roy. Meteor. Soc., 106, 447–462, 1980.

Glahn, H. R. and Lowry, D. A.: The use of model output statistics (MOS) in objective weather forecasting, J. Appl. Meteorol., 11, 1203–1211, 1972.

Hansen, J. W., Hodges, A. W., and Jones, J. W.: ENSO influences on agriculture in the southeastern United States*, J. Climate, 11, 404–411, 1998.

Ham, Y. G., Kug, J. S., Park, J. Y., and Jin, F. F.: Sea surface temperature in the north tropical Atlantic as a trigger for El Niño/Southern Oscillation events, Nat. Geosci., 6, 112–116, 2013a.

Ham, Y. G., Sung, M. K., An, S. I., Schubert, S. D., and Kug, J. S.: Role of tropical Atlantic SST variability as a modulator of El Niño teleconnections, Asia-Pacific, J. Atmos. Sci., 50, 247–261, 2013b.

Harris, I., Jones, P. D., Osborn, T. J., and Lister, D. H.: Updated high-resolution grids of monthly climatic observations–the CRU TS3. 10 Dataset, Int. J. Climatol., 34, 623–642, 2014.

Harrison, D. E. and Larkin, N. K.: El Niño–Southern Oscillation sea surface temperature and wind anomalies, 1946–1993, Rev. Geophys., 36, 353–399, 1998.

Hasselmann, K.: Stochastic climate models part I, theory. Tellus, 28, 473–485, 1976.

Haylock, M. R., Peterson, T. C., Alves, L. M., Ambrizzi, T., Anunciação, Y. M. T., Baez, J., and Vincent, L. A.: Trends in total and extreme South American rainfall in 1960–2000 and links with sea surface temperature, J. Climate, 19, 1490–1512, 2006.

Hsieh, W. W.: Nonlinear canonical correlation analysis of the tropical Pacific climate variability using a neural network approach, J. Climate, 14, 2528–2539, 2001.

Hsieh, W. W. and Tang, B.: Applying neural network models to prediction and data analysis in meteorology and oceanography, Bull. Am. Meteorol. Soc., 79, 1855–1870, doi:10.1175/1520-0477(1998)079<1855:ANNMTP>2.0.CO;2, 1998.

Janicot, S.: Spatiotemporal variability of West African rainfall, Part I: Regionalizations and typings, J. Climate, 5, 489–497, 1992.

Janicot, S., Moron, V., and Fontaine, B.: Sahel droughts and ENSO dynamics, Geophys. Res. Lett., 23, 515–518, 1996.

Janicot, S., Harzallah, A., Fontaine, B., and Moron, V.: West African monsoon dynamics and eastern equatorial Atlantic and Pacific SST anomalies (1970–88), J. Climate, 11, 1874–1882, 1998.

Janicot, S., Trzaska, S., and Poccard, I.: Summer Sahel-ENSO teleconnection and decadal time scale SST variations, Clim. Dynam., 18, 303–320, 2001.

Janowiak, J. E.: An investigation of interannual rainfall variability in Africa, J. Climate, 1, 240–255, 1988.

Ji, M., Kumar, A., and Leetmaa, A.: A multiseason climate forecast system at the National Meteorological Center, B. Am. Meteorol. Soc., 75, 569–577, 1994a.

Ji, M., Kumar, A., and Leetmaa, A.: An experimental coupled forecast system at the National Meteorological Center, Tellus A, 46, 398–418, 1994b.

Joly, M. and Voldoire, A.: Influence of ENSO on the West African monsoon: temporal aspects and atmospheric processes, J. Climate, 22, 3193–3210, 2009.

Keenlyside, N. S., Ding, H., and Latif, M.: Potential of equatorial Atlantic variability to enhance El Niño prediction, Geophys. Res. Lett., 40, 2278–2283, 2013.

Klein, W. H. and Glahn, H. R.: Forecasting local weather by means of model output statistics, B. Am. Meteorol. Soc., 55, 1217–1227, 1974.
Klein, S. A., Soden, B. J., and Lau, N. C.: Remote sea surface temperature variations during ENSO: evidence for a tropical atmospheric bridge, J. Climate, 12, 917–932, 1999.
Knutti, R., Stocker, T. F., Joos, F., and Plattner, G. K.: Probabilistic climate change projections using neural networks, Clim. Dynam., 21, 257–272, 2003.
Korecha, D. and Barnston, A. G.: Predictability of June–September rainfall in Ethiopia, Mon. Weather Rev., 135, 628–650, 2007.
Kovats, R. S.: El Niño and human health, B. World Health Organ., 78, 1127–1135, 2000.
Kovats, R. S., Bouma, M. J., Hajat, S., Worrall, E., and Haines, A.: El Niño and health, Lancet, 362, 1481–1489, 2003.
Kucharski, F., Bracco, A., Yoo, J. H., and Molteni, F.: Atlantic forced component of the Indian monsoon interannual variability, Geophys. Res. Lett., 35, L04706, doi:10.1029/2007GL033037, 2008.
Latif, M. and Barnett, T. P.: Interactions of the tropical oceans, J. Climate, 8, 952–964, 1995.
Legates, D. R. and Willmott, C. J.: Mean seasonal and spatial variability in gauge-corrected, global precipitation, Int. J. Climatol., 10, 111–127, 1990.
Legler, D. M., Bryant, K. J., and O'Brien, J. J.: Impact of ENSO-related climate anomalies on crop yields in the US, Climatic Change, 42, 351–375, 1999.
Li, G. and Xie, S. P.: Origins of tropical-wide SST biases in CMIP multi-model ensembles, Geophys. Res. Lett., 39, L22703, doi:10.1029/2012GL053777, 2012.
Li, G. and Xie, S. P.: Tropical biases in CMIP5 multimodel ensemble: the excessive equatorial Pacific cold tongue and double ITCZ problems*, J. Climate, 27, 1765–1780, 2014.
Li, Z. and Kafatos, M.: Interannual variability of vegetation in the United States and its relation to El Nino/Southern Oscillation, Remote Sens. Environ., 71, 239–247, 2000.
Lin, J. L.: The double-ITCZ problem in IPCC AR4 coupled GCMs: ocean–atmosphere feedback analysis, J. Climate, 20, 4497–4525, 2007.
Linthicum, K. J., Anyamba, A., Chretien, J. P., Small, J., Tucker, C. J., and Britch, S. C.: The role of global climate patterns in the spatial and temporal distribution of vector-borne disease, in: Vector Biology, Ecology and Control, Springer, the Netherlands, 3–13, 2010.
Livezey, R. E. and Chen, W. Y.: Statistical field significance and its determination by Monte Carlo techniques, Mon. Weather Rev., 111, 46–59, 1983.

GMDD
8, 3971–4018, 2015

S^4CAST seasonal forecast model

R. Suárez-Moreno and B. Rodríguez-Fonseca

López-Parages, J. and Rodríguez-Fonseca, B.: Multidecadal modulation of El Niño influence on the Euro-Mediterranean rainfall, Geophys. Res. Lett., 39, L02704, doi:10.1029/2011GL050049, 2012.

López-Parages, J., Rodrígez-Fonseca, B., and Terray, L.: A mechanism for the multidecadal modulation of ENSO teleconnections with Europe, Clim. Dynam., 1–14, doi:10.1007/s00382-014-2319-x, 2014.

Losada, T., Rodríguez-Fonseca, B., Polo, I., Janicot, S., Gervois, S., Chauvin, F., and Ruti, P.: Tropical response to the Atlantic Equatorial mode: AGCM multimodel approach, Clim. Dynam., 35, 45–52, 2010a.

Losada, T., Rodríguez-Fonseca, B., Janicot, S., Gervois, S., Chauvin, F., and Ruti, P.: A multi-model approach to the Atlantic Equatorial mode: impact on the West African monsoon, Clim. Dynam., 35, 29–43, 2010b.

Losada, T., Rodríguez-Fonseca, B., Mohino, E., Bader, J., Janicot, S., and Mechoso, C. R.: Tropical SST and Sahel rainfall: a non-stationary relationship, Geophys. Res. Lett., 39, L12705, doi:10.1029/2012GL052423, 2012.

Lu, J.: The dynamics of the Indian Ocean sea surface temperature forcing of Sahel drought, Clim. Dynam., 33, 445–460, 2009.

Maia, A. H., Meinke, H., Lennox, S., and Stone, R.: Inferential, nonparametric statistics to assess the quality of probabilistic forecast systems, Mon. Weather Rev., 135, 351–362, 2007.

Majda, A. J., Timofeyev, I., and Eijnden, E. V.: Models for stochastic climate prediction, P. Natl. Acad. Sci. USA, 96, 14687–14691, 1999.

Martin, E. R. and Thorncroft, C. D.: The impact of the AMO on the West African monsoon annual cycle, Q. J. Roy. Meteor. Soc., 140, 31–46, 2013.

Martín-Rey, M., Polo, I., Rodríguez-Fonseca, B., and Kucharski, F.: Changes in the interannual variability of the tropical Pacific as a response to an equatorial Atlantic forcing, Sci. Mar., 76, 105–116, 2012.

Martín-Rey, M., Rodríguez-Fonseca, B., Polo, I., and Kucharski, F.: On the Atlantic–Pacific Niños connection: a multidecadal modulated mode, Clim. Dynam., 43, 3163–3178, 2014.

Mason, S. J., Goddard, L., Graham, N. E., Yulaeva, E., Sun, L., and Arkin, P. A.: The IRI seasonal climate prediction system and the 1997/98 El Niño event, B. Am. Meteorol. Soc., 80, 1853–1873, 1999.

Michaelsen, J.: Cross-validation in statistical climate forecast models, J. Clim. Appl. Meteorol., 26, 1589–1600, 1987.

McMichael, A. J., Woodruff, R. E., and Hales, S.: Climate change and human health: present and future risks, Lancet, 3367, 859–869, doi:10.1016/S0140-6736(06)68079-3, 2006.

Mokhov, I. I. and Smirnov, D. A.: El Niño–Southern Oscillation drives North Atlantic Oscillation as revealed with nonlinear techniques from climatic indices, Geophys. Res. Lett., 33, L03708, doi:10.1029/2005GL024557, 2006.

Mohino, E., Janicot, S., and Bader, J.: Sahel rainfall and decadal to multi-decadal sea surface temperature variability, Clim. Dynam., 37, 419–440, 2011.

Naylor, R. L., Falcon, W. P., Rochberg, D., and Wada, N.: Using El Nino/Southern Oscillation climate data to predict rice production in Indonesia, Climatic Change, 50, 255–265, 2001.

Newman, M. and Sardeshmukh, P. D.: A caveat concerning singular value decomposition, J. Climate, 8, 352–360, 1995.

Nnamchi, H. C. and Li, J.: Influence of the South Atlantic Ocean dipole on West African summer precipitation, J. Climate, 24, 1184–1197, 2011.

Nnamchi, H. C., Li, J., and Anyadike, R. N.: Does a dipole mode really exist in the South Atlantic Ocean?, J. Geophys. Res.-Atmos., 116, D15104, doi:10.1029/2010JD015579, 2011.

Palmer, T. N.: Influence of the Atlantic, Pacific and Indian oceans on Sahel rainfall, Nature, 322, 251–253, doi:10.1038/322251a0, 1986.

Patz, J. A.: A human disease indicator for the effects of recent global climate change, P. Natl. Acad. Sci. USA, 99, 12506–12508, 2002.

Patz, J. A., Campbell-Lendrum, D., Holloway, T., and Foley, J. A.: Impact of regional climate change on human health, Nature, 438, 310–317, 2005.

Penland, C. and Matrosova, L.: Prediction of tropical Atlantic sea surface temperatures using linear inverse modeling, J. Climate, 11, 483–496, 1998.

Penland, C. and Sardeshmukh, P. D.: The optimal growth of tropical sea surface temperature anomalies, J. Climate, 8, 1999–2024, 1995.

Phillips, J. G., Cane, M. A., and Rosenzweig, C.: ENSO, seasonal rainfall patterns and simulated maize yield variability in Zimbabwe, Agr. Forest Meteorol., 90, 39–50, 1998.

Podestá, G. P., Messina, C. D., Grondona, M. O., and Magrin, G. O.: Associations between grain crop yields in central-eastern Argentina and El Niño–Southern Oscillation, J. Appl. Meteorol., 38, 1488–1498, 1999.

Polo, I., Rodríguez-Fonseca, B., Losada, T., and García-Serrano, J.: Tropical Atlantic variability modes (1979–2002), Part I: Time-evolving SST modes related to West African rainfall, J. Climate, 21, 6457–6475, 2008.

Polo, I., Martin-Rey, M., Rodríguez-Fonseca, B., Kucharski, F., and Mechoso, C. R.: Processes in the Pacific La Niña onset triggered by the Atlantic Niño, Clim. Dynam., 44, 115–131, doi:10.1007/s00382-014-2354-7, 2014.

Rasmusson, E. M. and Carpenter, T. H.: Variations in tropical sea surface temperature and surface wind fields associated with the Southern Oscillation/El Niño, Mon. Weather Rev., 110, 354–384, 1982.

Rasmusson, E. M. and Carpenter, T. H.: The relationship between eastern equatorial Pacific sea surface temperatures and rainfall over India and Sri Lanka, Mon. Weather Rev., 111, 517–528, 1983.

Rayner, N. A., Parker, D. E., Horton, E. B., Folland, C. K., Alexander, L. V., Rowell, D. P., and Kaplan, A.: Global analyses of sea surface temperature, sea ice, and night marine air temperature since the late nineteenth century, J. Geophys. Res.-Atmos., 108, 4407, doi:10.1029/2002JD002670, 2003.

Recalde-Coronel, G. C., Barnston, A. G., Muñoz, and Á. G.: Predictability of December–April rainfall in coastal and andean Ecuador, J. Appl. Meteorol. Clim., 53, 1471–1493, doi:10.1175/JAMC-D-13-0133.1, 2014.

Richter, I. and Xie, S. P.: On the origin of equatorial Atlantic biases in coupled general circulation models, Clim. Dynam., 31, 587–598, 2008.

Richter, I., Xie, S. P., Wittenberg, A. T., and Masumoto, Y.: Tropical Atlantic biases and their relation to surface wind stress and terrestrial precipitation, Clim. Dynam., 38, 985–1001, 2012.

Rodríguez-Fonseca, B., Polo, I., García-Serrano, J., Losada, T., Mohino, E., Mechoso, C. R., and Kucharski, F.: Are Atlantic Niños enhancing Pacific ENSO events in recent decades?, Geophys. Res. Lett., 36, L20705, doi:10.1029/2009GL040048, 2009.

Rodríguez-Fonseca, B., Janicot, S., Mohino, E., Losada, T., Bader, J., Caminade, C., and Voldoire, A.: Interannual and decadal SST-forced responses of the West African monsoon, Atmos. Sci. Lett., 12, 67–74, 2010.

Rodríguez-Fonseca, B., Mohino, E., Mechoso C. R., Caminade, C., Biasutti, M., Gaetani, M., García-Serrano, J., Vizy, E. K., Cook, K., Xue, Y., Polo, I., Losada, L., Druyan L,. Fontaine, B., Bader, J., Doblas-Reyes, F. J., Goddard, L., Janicot, S., Arribas, A., Lau, W., Colman, A., Vellinga, M., Rowell, D. P., Kucharski, F., and Voldoire, A.: Variability and predictability of West African droughts, a review on the role of sea surface temperature anomalies, J. Climate, 28, 4034–4060, doi:10.1175/JCLI-D-14-00130.1, 2015.

GMDD
8, 3971–4018, 2015

R. Suárez-Moreno and B. Rodríguez-Fonseca

Roe, G. H. and Steig, E. J.: Characterization of millennial-scale climate variability, J. Climate, 17, 1929–1944, 2004.
Rowell, D. P.: Teleconnections between the tropical Pacific and the Sahel, Q. J. Roy. Meteor. Soc., 127, 1683–1706, 2001.
Rowell, D. P.: The impact of Mediterranean SSTs on the Sahelian rainfall season, J. Climate, 16, 849–862, 2003.
Rudolf, B., Becker, A., Schneider, U., Meyer-Christoffer, A., and Ziese, M.: The new "GPCC Full Data Reanalysis Version 5" providing high-quality gridded monthly precipitation data for the global land-surface is public available since December 2010, GPCC status report December, GPCC Technical Report, available at: gpcc.dwd.de (last access: 15 January 2011), 2010.
Saravanan, R. and Chang, P.: Interaction between tropical Atlantic variability and El Nino-southern oscillation, J. Climate, 13, 2177–2194, 2000.
Schneider, U., Becker, A., Finger, P., Meyer-Christoffer, A., Ziese, M., and Rudolf, B.: GPCC's new land surface precipitation climatology based on quality-controlled in situ data and its role in quantifying the global water cycle, Theor. Appl. Climatol., 115, 15–40, 2014.
Schurer, A. P., Hegerl, G. C., Mann, M. E., Tett, S. F., and Phipps, S. J.: Separating forced from chaotic climate variability over the past millennium, J. Climate, 26, 6954–6973, 2013.
Shin, S. I., Sardeshmukh, P. D., and Webb, R. S.: Optimal tropical sea surface temperature forcing of North American drought, J. Climate, 23, 3907–3917, 2010.
Smith, T. M. and Reynolds, R. W.: Extended reconstruction of global sea surface temperatures based on COADS data (1854–1997), J. Climate, 16, 1495–1510, 2003.
Smith, T. M. and Reynolds, R. W.: Improved extended reconstruction of SST (1854–1997), J. Climate, 17, 2466–2477, 2004.
Smith, T. M., Reynolds, R. W., Peterson, T. C., and Lawrimore, J.: Improvements to NOAA's historical merged land-ocean surface temperature analysis (1880–2006), J. Climate, 21, 2283–2296, 2008.
Shukla, R. P., Tripathi, K. C., Pandey, A. C., and Das, I. M. L.: Prediction of Indian summer monsoon rainfall using Niño indices: a neural network approach, Atmos. Res., 102, 99–109, 2011.
Tang, B., Hsieh, W. W., Monahan, A. H., and Tangang, F. T.: Skill comparisons between neural networks and canonical correlation analysis in predicting the equatorial Pacific sea surface temperatures, J. Climate, 13, 287–293, 2000.

Tao, F., Yokozawa, M., Zhang, Z., Hayashi, Y., Grassl, H., and Fu, C.: Variability in climatology and agricultural production in China in association with the East Asian summer monsoon and El Niño Southern Oscillation, Clim. Res., 28, 23–30, 2004.

Toniazzo, T. and Woolnough, S.: Development of warm SST errors in the southern tropical Atlantic in CMIP5 decadal hindcasts, Clim. Dynam., 43, 2889–2913, doi:10.1007/s00382-013-1691-2, 2013.

Travasso, M. I., Magrin, G. O., Grondona, M. O., and Rodríguez, G. R.: The use of SST and SOI anomalies as indicators of crop yield variability, Int. J. Climatol., 29, 23–29, 2009.

Trenberth, K. E., Caron, J. M., Stepaniak, D. P., and Worley, S.: Evolution of El Niño–Southern Oscillation and global atmospheric surface temperatures, J. Geophys. Res.-Atmos., 107, AAC-5, doi:10.1029/2000JD000298, 2002.

Van den Dool, H. M.: Searching for analogues, how long must we wait?, Tellus A, 46, 314–324, 1994.

Vannière, B., Guilyardi, E., Madec, G., Doblas-Reyes, F. J., and Woolnough, S.: Using seasonal hindcasts to understand the origin of the equatorial cold tongue bias in CGCMs and its impact on ENSO, Clim. Dynam., 40, 963–981, 2013.

Verdin, J., Funk, C., Klaver, R., and Roberts, D.: Exploring the correlation between Southern Africa NDVI and Pacific sea surface temperatures: results for the 1998 maize growing season, Int. J. Remote Sens., 20, 2117–2124, 1999.

Vimont, D. J.: Analysis of the Atlantic meridional mode using linear inverse modeling: seasonality and regional influences, J. Climate, 25, 1194–1212, 2012.

Vislocky, R. L. and Fritsch, J. M.: Improved model output statistics forecasts through model consensus, B. Am. Meteorol. Soc., 76, 1157–1164, 1995.

Wahl, S., Latif, M., Park, W., and Keenlyside, N.: On the tropical Atlantic SST warm bias in the Kiel Climate Model, Clim. Dynam., 36, 891–906, 2011.

Wallace, J. M., Smith, C., and Bretherton, C. S.: Singular value decomposition of wintertime sea surface temperature and 500-mb height anomalies, J. Climate, 5, 561–576, 1992.

Wang, S. Y., L'Heureux, M., and Chia, H. H.: ENSO prediction one year in advance using western North Pacific sea surface temperatures, Geophys. Res. Lett., 39, L05702, doi:10.1029/2012GL050909, 2012.

Ward, M. N.: Diagnosis and short-lead time prediction of summer rainfall in tropical North Africa at interannual and multidecadal timescales, J. Climate, 11, 3167–3191, 1998.

Widmann, M.: One-dimensional CCA and SVD, and their relationship to regression maps, J. Climate, 18, 2785–2792, 2005.
Xue, Y., Chen, M., Kumar, A., Hu, Z. Z., and Wang, W.: Prediction skill and bias of tropical Pacific sea surface temperatures in the NCEP Climate Forecast System version 2, J. Climate, 26, 5358–5378, 2013.
Zebiak, S. E. and Cane, M. A.: A model El Niño–Southern Oscillation, Mon. Weather Rev., 115, 2262–2278, 1987.

GMDD
8, 3971–4018, 2015

S[4]CAST seasonal forecast model

R. Suárez-Moreno and B. Rodríguez-Fonseca

Table 1. Case studies (EP-SL0, EP-SL1, SC-SL0, SC-SL1, NSC-SL0, NSC-SL1) corresponding to the model simulations developed in this work depending on predictand and predictor selections.

				Periods of stationarity		
				Non-stationary	Stationary	
				EP[1]	SC[2]	NSC[2]
Predictor	Lead-time 0	AMJ	SL0[3]	EP-SL0	SC-SL0	NSC-SL0
selections	Synchronous + partial overlap	MJJ + JJA + JAS	SL1[4]	EP-SL1	SC-SL1	NSC-SL1

[1] Non-stationary period referred to the selection of the Entire Period (EP) for statistical analysis.
[2] Stationary periods determined by significant correlation using 21 years moving correlation windows. Obtained periods are the Significant Correlation period (SC) and No-Significant Correlation period (NSC).
[3] Selection 0 (SL0): Seasonal period for the predictor at lead-time = 0 (April–May–June; AMJ).
[4] Selection 1 (SL1): Seasonal periods for the predictor at synchronous season and partial monthly overlaps (May–June–July MJJ, June–July–August JJA and July–August–September JAS).

GMDD
8, 3971–4018, 2015

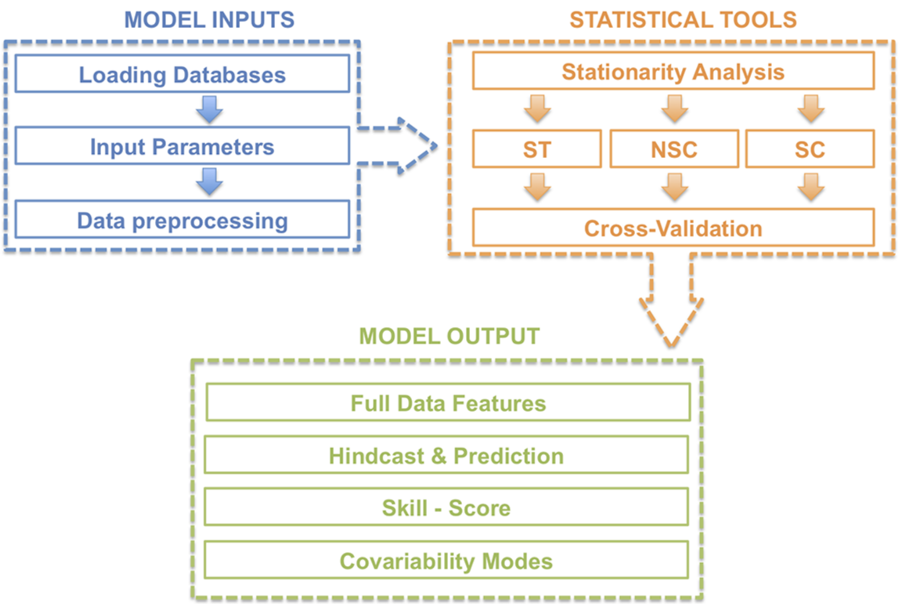

Figure 1. Schematic diagram illustrating the structure of the model.

GMDD
8, 3971–4018, 2015

Title Page
Abstract | Introduction
Conclusions | References
Tables | Figures
◀| |▶
◀ ▶
Back | Close
Full Screen / Esc
Printer-friendly Version
Interactive Discussion

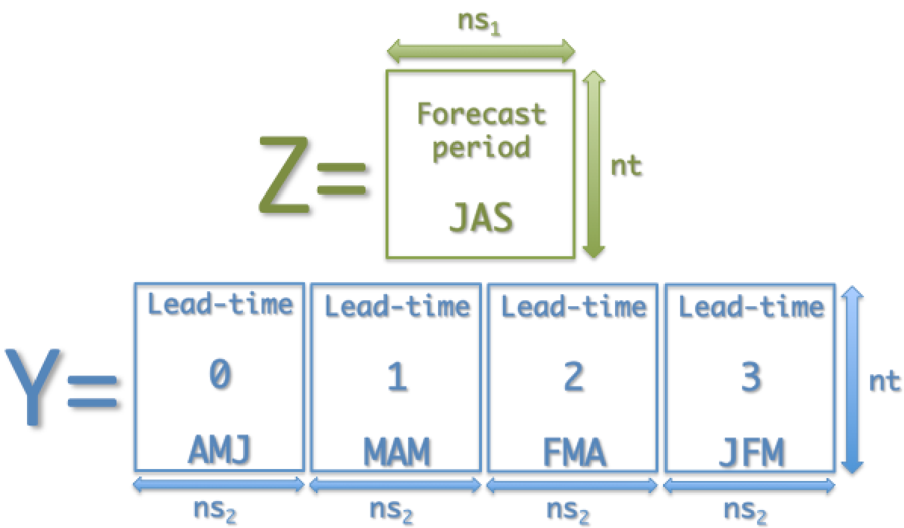

Figure 2. Predictand (Z) and predictor (Y) fields represented by their corresponding data matrices. The illustration relates to an example in which the forecast period covers the months July–August–September (JAS) and the predictor is selected for four distinct seasons: January–February–March (JFM, lead-time = 3); February–March–April (FMA, lead-time = 2); March–April–May (MAM, lead-time = 1); April-May-June (AMJ, lead-time = 0). Each of these submatrices for the predictor has the same temporal dimension (nt) and spatial dimension (ns_2). The predictand may have a different spatial dimension (ns_1) but the same temporal dimension (nt) to enable matrix calculations required by MCA methodology.

GMDD
8, 3971–4018, 2015

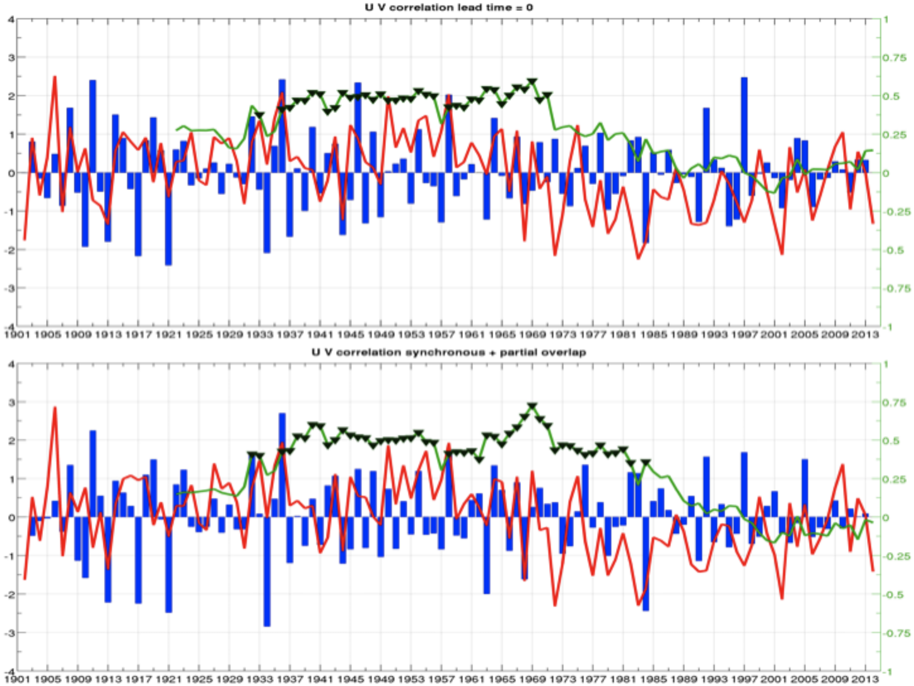

Figure 3. 21 years moving correlation windows (green line) between the expansion coefficients *U* corresponding to predictor field (SSTA, blue bars) and *V* corresponding to predictand field (anomalous rainfall, red line) obtained from the leading mode of co-variability from MCA analysis between both anomalous fields. Top panel correspond to the analysis considering SL0 for predictor; bottom panel refers to SL1 (see Table 1). Shaded triangles indicate significant correlation under a Montecarlo Test at 90 %.

GMDD
8, 3971–4018, 2015

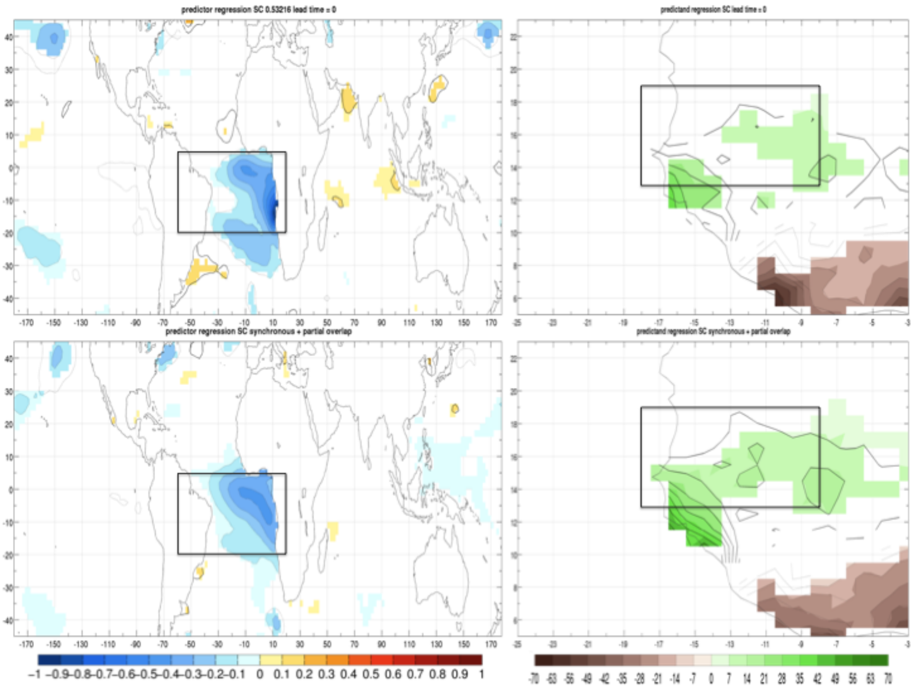

Figure 4. Regression maps obtained from the leading MCA (SC period) done between SSTA in the Atlantic and western Sahel rainfall. Left column represents the homogeneous regression map done projecting the expansion coefficient $\boldsymbol{U}$ onto global SSTA (°C std^{-1}). Right column represents the heterogeneous regression map done projecting expansion coefficient $\boldsymbol{U}$ onto the anomalous Sahelian rainfall (mm day^{-1} std^{-1}). Cases SC-SL0 (top panels) and SC-SL1 (bottom panels) are presented (see Table 1). Rectangles show the selected regions for predictor and predictand variables considered in the MCA analysis. Values are plotted in regions where statistical significance under a Montecarlo test is higher than 90 %.

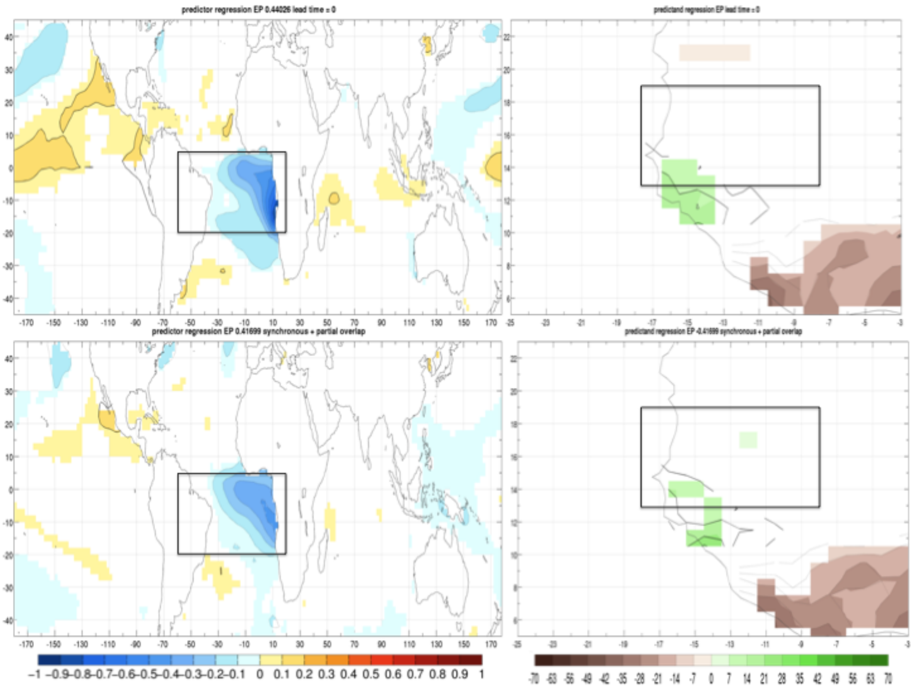

Figure 5. Regression maps obtained from the leading MCA (EP period) done between SSTA in the Atlantic and western Sahel rainfall. Left column represents the homogeneous regression map done projecting the expansion coefficient ***U*** onto global SSTA (°C std^{-1}). Right column represents the heterogeneous regression map done projecting expansion coefficient ***U*** onto the anomalous Sahelian rainfall (mm day^{-1} std^{-1}). Cases EP-SL0 (top panels) and EP-SL1 (bottom panels) are presented (see Table 1). Rectangles show the selected regions for predictor and predictand variables considered in the MCA analysis. Values are plotted in regions where statistical significance under a Montecarlo test is higher than 90 %.

Title Page
Abstract
Introduction
Conclusions
References
Tables
Figures
◂
▸
Back
Close
Full Screen / Esc
Printer-friendly Version
Interactive Discussion

GMDD

8, 3971–4018, 2015

Title Page

Abstract | Introduction

Conclusions | References

Tables | Figures

◀| |▶

◀ ▶

Back | Close

Full Screen / Esc

Printer-friendly Version

Interactive Discussion

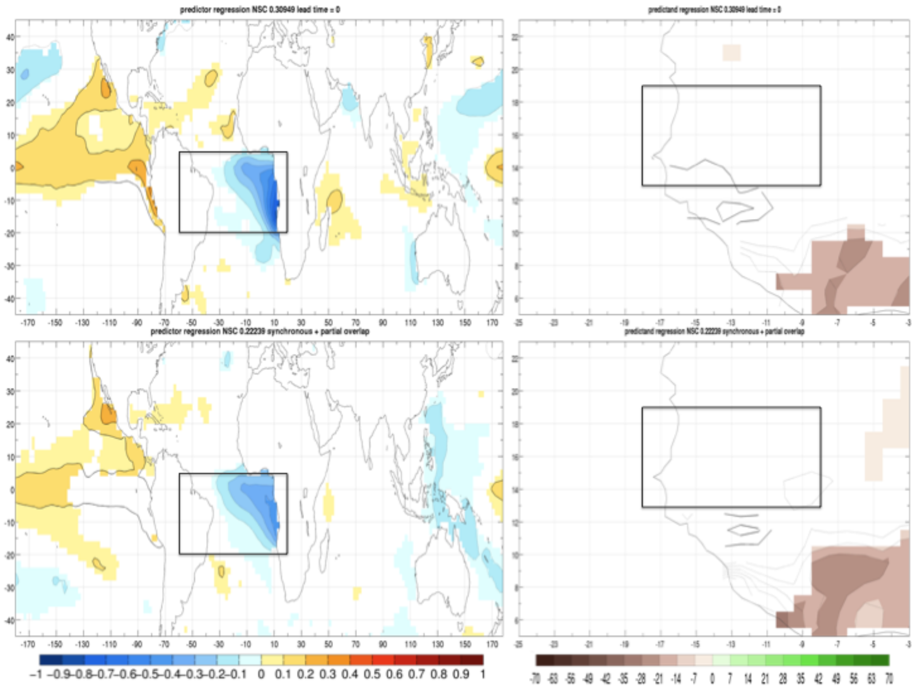

Figure 6. Regression maps obtained from the leading MCA (NSC period) done between SSTA in the Atlantic and western Sahel rainfall. Left column represents the homogeneous regression map done projecting the expansion coefficient ***U*** onto global SSTA (°C std^{-1}). Right column represents the heterogeneous regression map done projecting expansion coefficient ***U*** onto the anomalous Sahelian rainfall (mm day^{-1} std^{-1}). Cases NSC-SL0 (top panels) and NSC-SL1 (bottom panels) are presented (see Table 1). Rectangles show the selected regions for predictor and predictand variables considered in the MCA analysis. Values are plotted in regions where statistical significance under a Montecarlo test is higher than 90 %.

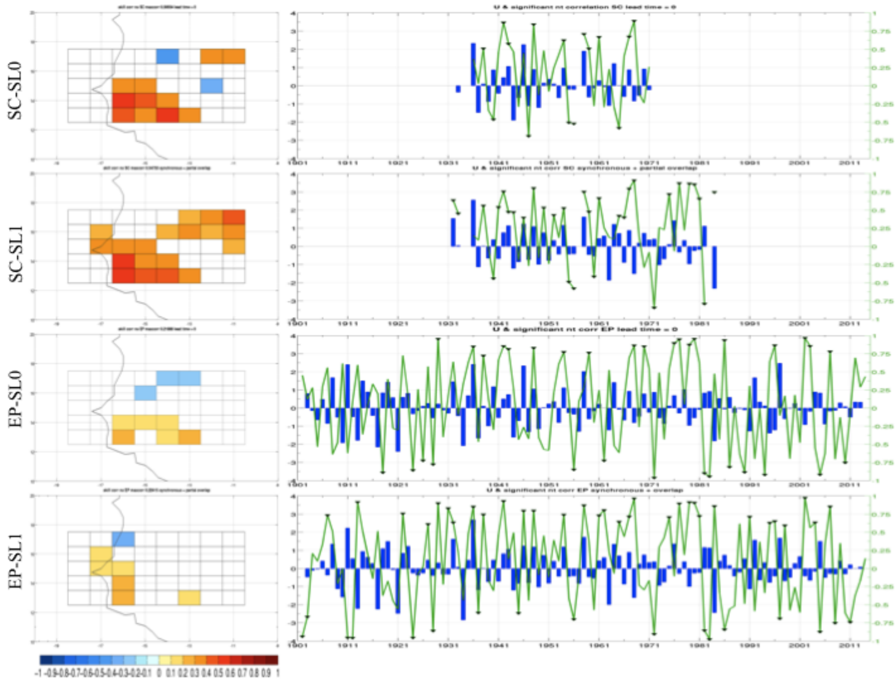

Figure 7. Skill-score validation in terms of Pearson correlation coefficients between observed and simulated maps (hindcast). Left column corresponds to the spatial validation for each point in space. The right column corresponds to validation time series (green line) between hindcasts and observations considering only the regions indicated by significant spatial correlation. Significant correlation values for time series are indicated by shaded triangles. Blue bars correspond to the expansion coefficient (U) of the SSTA (predictor). The rows correspond to the SC and EP case studies disaggregated in Table 1. Significant values are plotted from 90 % of statistical significance under a Montecarlo test.

GMDD
8, 3971–4018, 2015

R. Suárez-Moreno and B. Rodríguez-Fonseca

Title Page
Abstract | Introduction
Conclusions | References
Tables | Figures
◂◂ | ▸▸
◂ | ▸
Back | Close
Full Screen / Esc
Printer-friendly Version
Interactive Discussion

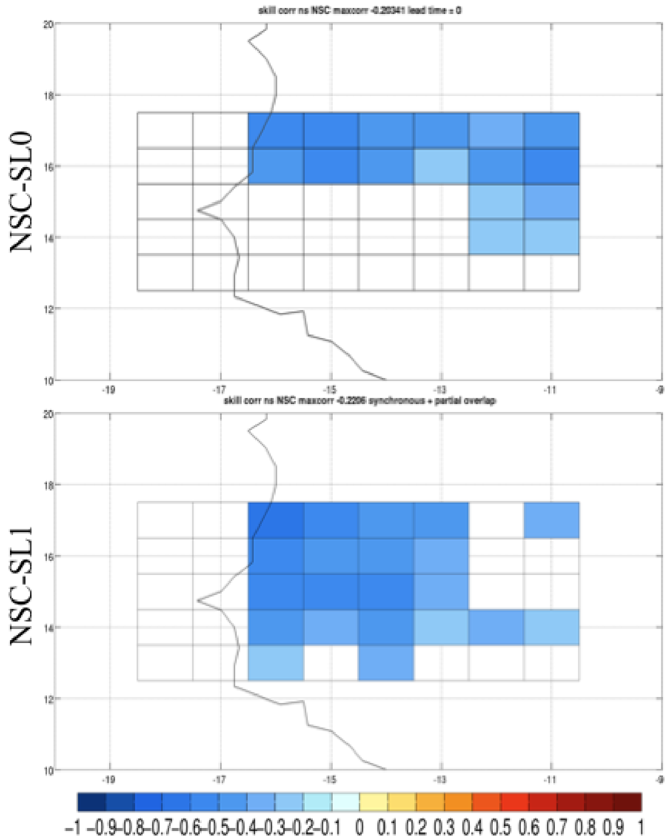

Figure 8. Spatial validation in terms of Pearson correlation coefficients between observed and simulated maps (hindcast) for each point in space. Each row corresponds to a case study within NSC period disaggregated in Table 1. Significant values are plotted from 90 % of statistical significance under a Montecarlo test.

GMDD
8, 3971–4018, 2015

S^{4}CAST seasonal forecast model

R. Suárez-Moreno and B. Rodríguez-Fonseca

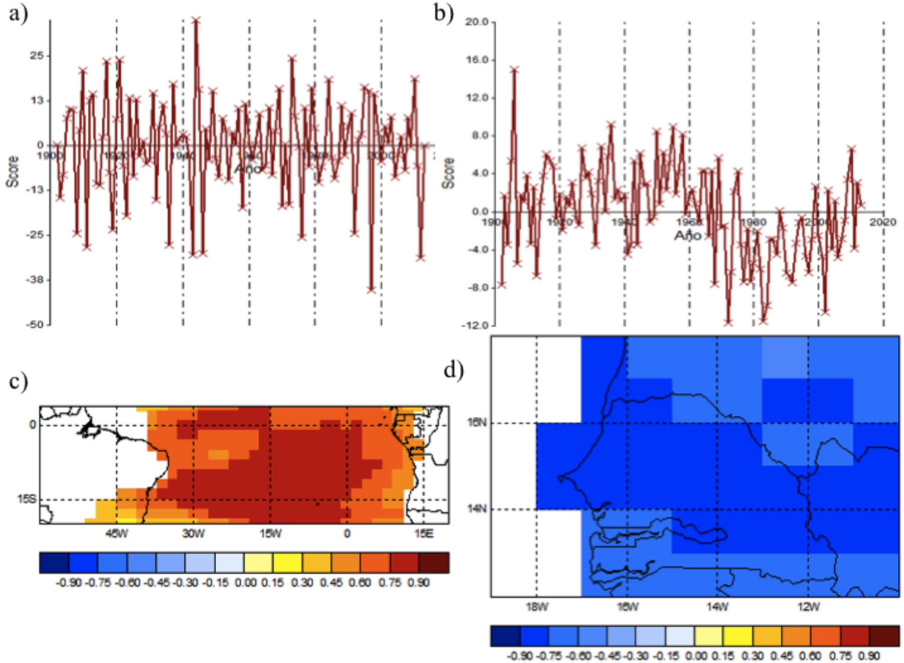

Figure 9. Leading mode from CCA analysis using the Climate Predictability Tool (CPT) between the predictor field (Y) corresponding to SSTA in the tropical Atlantic (20° S–4° N/60° W–20° E) and the predictand (Z) in the western Sahel (12.5–17.5° N/17.5–9.5° W). **(a)** Time series of the predictor expansion coefficient and **(b)** the predictand expansion coefficient. **(c)** Correlation maps corresponding to the predictor and **(d)** the predictand.

GMDD
8, 3971–4018, 2015

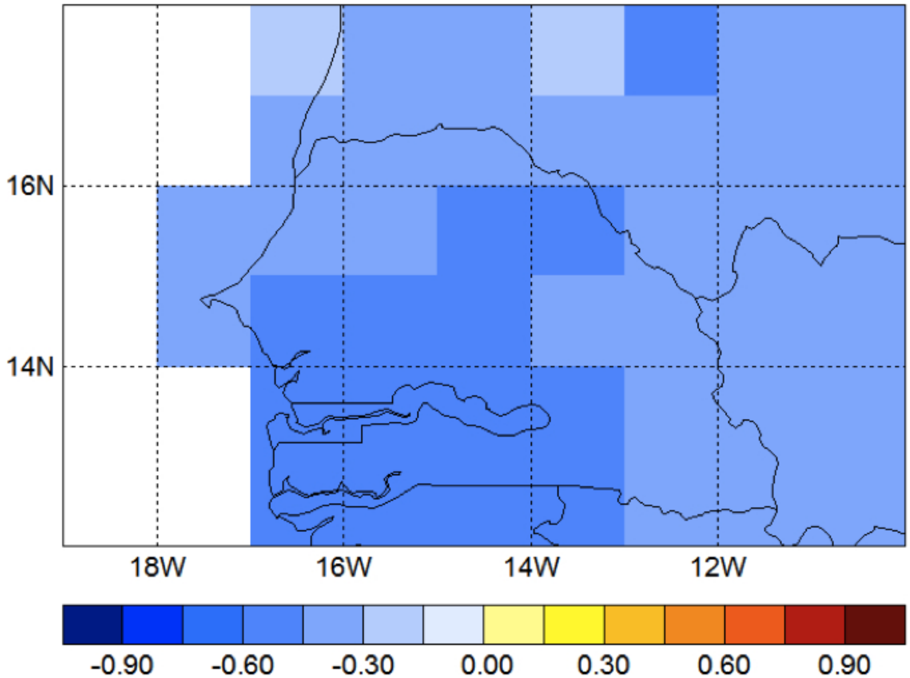

Figure 10. Validation map from CPT by using Pearson correlation coefficients between each spatial point of the hindcasts and observed maps for the entire study period (1902–2013).

GMDD

8, 3971–4018, 2015

S^{4}CAST seasonal forecast model

R. Suárez-Moreno and B. Rodríguez-Fonseca